Polaron solutions and normal-mode analysis in the semiclassical Holstein model

G. Kalosakas
Physics Department, University of Crete and Foundation for Research and Technology–Hellas, P.O. Box 2208, 71003 Heraklion-Crete, Greece

S. Aubry
Physics Department, University of Crete and Foundation for Research and Technology–Hellas, P.O. Box 2208, 71003 Heraklion-Crete, Greece
and Laboratoire Léon Brillouin, Centre d'Etudes Nucléaires de Saclay, 91191 Gif-Sur-Yvette, Cedex, France

G. P. Tsironis
Physics Department, University of Crete and Foundation for Research and Technology–Hellas, P.O. Box 2208, 71003 Heraklion-Crete, Greece

(Received 2 July 1997; revised manuscript received 19 November 1997)

We investigate polaron properties in the semiclassical Holstein model in one, two, and three dimensions, using two methods: a simple and efficient numerical scheme and a variational approach. We obtain accurate information on the energy and the existence regimes of the polaron state. We study small oscillations of the polaron through normal-mode analysis, investigate their stability, and evaluate the density of states of the polaron eigenfrequencies for different system parameters. The normal-mode analysis shows in the one-dimensional case a pinning-breathing mode crossing in the transition region of the small to large polaron. Similar crossings do not exist in higher dimensions. [S0163-1829(98)07329-9]

I. INTRODUCTION AND THE SEMICLASSICAL HOLSTEIN MOLEL

Polarons, of either purely electronic or excitonic nature, are ubiquitous in materials where the electron-phonon coupling cannot be ignored. Issues related to the formation and dynamics of polarons have been in the foreground of research for approximately half a century, during which several models were introduced and a variety of exact and approximate solution schemes have been tried.[1–16] The Holstein model has emerged as one of the fundamental models in the attempt to understand the fundamentals of polarons in condensed matter and biological systems. One of the most successful approaches for obtaining polaron ground state properties via the Holstein model has been through the use of scaling ideas and a continuous approximation. These studies showed that while in one dimension the polaron was always the ground state of the Holstein model in two and three dimensions, a minimal electon-phonon coupling is required for the phenomenon of the electronic wave function self-trapping that leads to polaron formation. Furthermore, while in one dimension there is a continuous crossover from the small to the large polaron, in two and three dimensions small coupling polarons do not exist. Most of the results of Ref. 3 have been shown to be correct also in the discrete limit.[9,10] In the present paper, one of our aims will be to readdress the well known stationary polaron properties, using, however, alternative approaches.

For our study we will use the semiclassical Holstein model, in which the lattice oscillators are treated classically. The dynamical equations of motion describe in the semiclassical approximation a quantum electron (or exciton) interacting with classical Einstein oscillators in a d-dimensional lattice. Polarons, which are localized stationary solutions of the equations of motion, will be calculated via a fast numerical scheme that enables us to evaluate the polaron wave function and its energy. The strength of this method is that while it is very simple it provides very accurate and easily obtainable information on polaron properties. Subsequently, we develop a variational method that gives accurate exact results for the critical values of the coupling parameter that determines the polaron regimes in one, two, and three dimensions (3D). We also derive analytical expressions for the small polaron energy that are in good agreement with the numerical results in 2D and 3D as well as in 1D for large enough coupling. The stationary polaron results will be used in Sec. III, where the polaron normal-modes are calculated through linearization of the equations of motion for the stationary polaron solutions. We focus on the lower frequency eigenmodes and discuss their character, i.e. the contribution of the electronic and phononic degrees of freedom. Furthermore, we present the total picture of the density of states for the spectrum of the polaron eigenfrequencies. We conclude our study in Sec. IV.

A. The semiclassical Holstein model

The Hamiltonian of the Holstein model consists of[1] $H_{tot}=H_{el}+H_{lat}+H_{int}$. The first term H_{el} describes a tight-binding electron in a d-dimensional simple lattice ($d=1$, 2, or 3) with N sites and periodic boundary conditions:

$$H_{el}=-V\sum_{m=1}^{N}\sum_{\delta[m]}|m\rangle\langle m+\delta|, \tag{1}$$

where the integer m counts all the lattice sites and the integer $\delta[m]$ of the second sum that depends on m denotes the sum-

mation of all the nearest neighbors at each site m (i.e., takes $2d$ values for $d=1,2,3$). The state $|m\rangle$ represents an atomiclike electronic state localized at site m, for example, a Wannier state. In Eq. (1) we have taken the on-site matrix element ϵ_0, appearing in the diagonal terms $\epsilon_0 \Sigma_m |m\rangle\langle m|$, to be zero, while $-V$ is the nearest-neighbor transfer integral.

The second term H_{lat} describes N identical Einstein oscillators, each located in a different lattice site and having mass M and frequency ω_0:

$$H_{lat}=\frac{1}{2M}\sum_{m=1}^{N} p_m^2+\frac{M\omega_0^2}{2}\sum_{m=1}^{N} x_m^2, \tag{2}$$

where p_m and x_m are the momentum and the displacement from the equilibrium, respectively, of the oscillator located at site m.

The last term H_{int} describes a local interaction of the electron with the optical lattice that is linear in the displacements of oscillators:

$$H_{int}=\chi\sum_{m=1}^{N} |m\rangle\langle m|x_m, \tag{3}$$

where χ is the electron-phonon coupling constant. This interaction term signifies that the on-site tight-binding matrix element ϵ_m, i.e., the local site energy, depends on the displacement of the oscillator at site m as $\epsilon_m=\epsilon_0+\chi x_m$.

We derive the equations of motion for this model by treating the oscillator subsystem classically, while we use a quantum description for the electron. This semiclassical treatment can be justified in cases of large atomic mass leading to very slow atomic motion compared to that of the electron. We write the electronic state as $|\Psi_e(t)\rangle=\Sigma_n C_n(t)|n\rangle$, where $C_n(t)$ is the probability amplitude to find the electron in the localized state $|n\rangle$. The Hamiltonian operator for the electron is $H_{el}+H_{int}$, given by Eqs. (1) and (3). Using the Schrödinger equation $i\hbar(d|\Psi_e\rangle/dt)=(H_{el}+H_{int})|\Psi_e\rangle$, we obtain the time evolution of the amplitudes $C_n(t)$:

$$i\hbar\frac{dC_n}{dt}=-V\left(\sum_{\delta[n]} C_{n+\delta}\right)+\chi C_n x_n. \tag{4}$$

The classical Hamiltonian that we use for the oscillators is given by $H_{clas}=\langle\Psi_e|H_{tot}|\Psi_e\rangle$. From the Hamilton equations $\dot{x}_n=\partial H_{clas}/\partial p_n$ and $\dot{p}_n=-\partial H_{clas}/\partial x_n$ we determine the dynamical behavior of the lattice variables. As a result we have

$$M\frac{d^2x_n}{dt^2}+M\omega_0^2 x_n+\chi|C_n|^2=0. \tag{5}$$

Similar equations, such as Eqs. (4) and (5), have been widely used in numerical studies of various electron-phonon systems.[17–21] In modified forms, they have also been studied in the Davydov's soliton model for the transport of vibrational energy in proteins.[22–25]

We use the dimensionless quantities $\tau=\omega_0 t$ (dimensionless time), $u_n=\sqrt{M\omega_0^2/V}x_n$ (dimensionless displacements), $k=\chi/\sqrt{VM\omega_0^2}$ [dimensionless effective coupling, designated usually as $\sqrt{\lambda}$ (Ref. 12)], and $\gamma=\hbar\omega_0/V=t_e/t_l$, where $t_e=\hbar/V$ and $t_l=1/\omega_0$ are the characteristic times for the motion of the electron and lattice, respectively. The parameter γ is also equal to $\alpha\sqrt{2(m^\star/M)}$, where $m^\star$ is the electronic band effective mass and $\alpha=a\sqrt{M\omega_0^2/V}$ is the dimensionless lattice constant (a is the lattice constant). Using these quantities we cast Eqs. (4) and (5) into a dimensionless form and obtain their dependence on only two parameters

$$i\gamma\frac{dC_n}{d\tau}=-\left(\sum_{\delta[n]} C_{n+\delta}\right)+kC_n u_n, \tag{6}$$

$$\frac{d^2u_n}{d\tau^2}+u_n+k|C_n|^2=0. \tag{7}$$

We also write for subsequent use the expressions for the dimensionless energies, given in units of V. The contribution of each term in the total energy $E_{tot}=E_{el}+E_{int}+E_{lat}$, where $E_{el}=\langle\Psi_e|H_{el}|\Psi_e\rangle$ and $E_{int}=\langle\Psi_e|H_{int}|\Psi_e\rangle$, is obtained through the relations

$$E_{el}=-\sum_{m=1}^{N}\sum_{\delta[m]} C_m^\star C_{m+\delta}, \tag{8}$$

$$E_{int}=k\sum_{m=1}^{N}|C_m|^2 u_m, \tag{9}$$

$$E_{lat}=\frac{1}{2}\sum_{m=1}^{N}\left(\frac{du_m}{d\tau}\right)^2+\frac{1}{2}\sum_{m=1}^{N}u_m^2. \tag{10}$$

In what follows we will study one-, two-, and three-dimensional polaron solutions of Eqs. (6) and (7), their stability properties analyzed through their normal-mode oscillations and their dependence on system parameters.

II. POLARON SOLUTIONS

A. Numerical scheme

The polarons are localized stationary solutions of the coupled system. In our case a stationary solution is obtained through $du_n/d\tau=0$ and $C_n(\tau)=\Psi_n e^{-i(E/\gamma)\tau}$, where Ψ_n is time independent. From Eq. (7) we have that for a stationary solution

$$u_n=-k|\Psi_n|^2 \tag{11}$$

and substituting in Eq. (6) we obtain for the electronic wave function

$$E\Psi_n=-\left(\sum_{\delta[n]}\Psi_{n+\delta}\right)-k^2|\Psi_n|^2\Psi_n. \tag{12}$$

This is the d-dimensional time-independent discrete nonlinear Schrödinger equation.[26–28] Equations (11) and (12), which describe the stationary solutions of the semiclassical model, are identical to those obtained in the adiabatic approximation.[1,9,10] The energy E that appears in Eq. (12) is equal to $E_{el}+E_{int}$, where now $E_{el}=-\Sigma_{m=1}^{N}\Sigma_{\delta[m]}\Psi_m^\star\Psi_{m+\delta}$ and $E_{int}=-k^2\Sigma_{m=1}^{N}|\Psi_m|^4$. In order to obtain the total energy of a stationary solution we have to add to E the lattice energy, i.e., $E_{tot}=E+E_{lat}$, where $E_{lat}=(k^2/2)\Sigma_{m=1}^{N}|\Psi_m|^4$.

The extended Bloch states $\Psi_n^q=(1/\sqrt{N})e^{iqn}$ are solutions of Eq. (12) forming a band with energies E from $-2d-k^2/N$ to $2d-k^2/N$, where d is the dimension of the lattice. The total energy, taking into account the lattice potential energy, is shifted by $+k^2/2N$. In the limit of an infinite chain the band is from $-2d$ to $2d$ and the lattice is undistorted. In addition to these extended states, Eq. (12) admits localized solutions as well. These localized electronic states accompanied by lattice distortions that are localized in the same area, as indicated by Eq. (11), represent polaron states.

A very simple method for the numerical calculation of polarons emerges from the fact that they are attractors of the map

$$\{\Psi\}\rightarrow\{\Psi'\}=H\{\Psi\}/\|H\{\Psi\}\|, \tag{13}$$

where $\{\Psi\}=(\Psi_1,\ldots,\Psi_N)$, the operator H is defined through Eq. (12) as

$$H\{\Psi\}_n=-\sum_{\delta[n]}\Psi_{n+\delta}-k^2|\Psi_n|^2\Psi_n,$$

and $\|H\{\Psi\}\|=\sqrt{\Sigma_{n=1}^N(H\{\Psi\}_n)^2}$ is the norm of the state $H\{\Psi\}$.[29]

It is easy to see that in the anti-integrable limit, defined as the limit where the electron does not move from site to site, i.e., the transfer integral $V\rightarrow 0$,[30,31] the term $\Sigma_{\delta[n]}\Psi_{n+\delta}$ of Eq. (12) is absent, and the on-site localized polaron is a very strong attractor of the map (13). When we depart from the nonintegrable limit this attractor becomes less strong, while in the two- and three-dimensional cases it is lost in some instances. In order to calculate the polaron state we begin with a completely localized initial state $\{\Psi^{init}\}_n=\delta_{n,n_0}$, act on this with the operator H, normalize the resulting vector, and repeat this procedure until convergence is achieved. As a result we find the polaron wave function $\{\Psi^{final}\}$, while the energy E of Eq. (12) is given through the norm $\|H\{\Psi^{final}\}\|$. This procedure converges very fast to the polaron state whenever it exists in most cases only after few tens of iterations, for an accuracy better than 10^{-10}. When there is no polaron solution it converges to the lowest energy extended state (except for the case $k=0$, where it cannot select between the lower and higher energy Bloch states).

The polaron solution depends only on the dimensionless effective coupling k and not on the parameter γ, as can be seen readily from Eqs. (12) and (11). The results we obtain are in agreement with those of Refs. 9 and 10 and summarized as follows. In 1D the polaron exists always as the ground state of the system and there is a smooth transition from the small polaron to the large polaron. Approximately we have a small (large) polaron for $k>2$ $(k<1)$. In the large polaron case the smaller the coupling k, the more extended in size and smaller in height the wave function. For example, for k of the order of 10^{-2} the size of the polaron is of the order of 10^3-10^4 lattice constants. It is therefore necessary to explore larger lattices in order to distinguish the polaron from the extended states. In a two-dimensional square lattice there are two critical values of the coupling $k_{c_1}=2.3877$ and $k_{c_2}=2.5844$ that determine three parameter regions: (i) for $k<k_{c_1}$ there is no polaron, (ii) for $k_{c_1}<k<k_{c_2}$ the polaron is metastable, i.e., has more energy than the corresponding lowest energy extended state, and (iii) for $k>k_{c_2}$ the polaron is the ground state of the system. Whenever the polaron exists, i.e., for $k>k_{c_1}$, it extends only to a few lattice sites, thus forming a small polaron. In a three-dimensional simple cubic lattice the picture is exactly the same as in 2D. The only difference is that now the critical values of coupling are shifted upward to $k_{c_1}=2.8022$ and $k_{c_2}=3.2887$.

Figures 1 and 2 summarize these findings. In Figs. 1(a)–1(c) the thick lines show the total polaron energy E_{tot} as a function of the effective coupling k for $d=1$, 2, and 3, respectively. Polaron wave functions are presented in Fig. 2. The thick continuous line in Fig. 2(a) shows a large one-dimensional polaron for $k=0.15$. The filled circles in Fig. 2(b) show a small polaron in 1D for $k=2.5$. Finally, the filled circles in Figs. 2(c) and 2(d) show sections of polarons in 2D for $k=2.5$ and in 3D for $k=4$, respectively.

B. Analytical variational results

We will consider simple trial functions that produce very accurate variational results. In three dimensions we have

$$\Psi_{m_x,m_y,m_z}=A\,\eta^{|m_x|+|m_y|+|m_z|}\quad\text{for } d=3, \tag{14}$$

where m_x refers to the site in the x direction, etc., and in lower dimensions the ansatz wave function changes appropriately. The variational parameter η takes values in the interval $0<\eta<1$ and gives the linear extent of the solution after the substitution $\eta=e^{-1/2\xi}$. As η increases the solution becomes more delocalized and in the limit $\eta\rightarrow 1$ we obtain an extended state. The coefficient A is evaluated through the normalization of the solution, i.e., $\Sigma_{m_x,\ldots}|\Psi_{m_x,\ldots}|^2=1$, leading to

$$A=\left(\frac{1-\eta^2}{1+\eta^2}\right)^{d/2}\quad\text{for } d=1,2,3. \tag{15}$$

The total variational energy Φ is given by

$$\Phi=-\sum_{m_x,\ldots}(\Psi^{\star}_{m_x,\ldots}\Psi_{m_x+1,\ldots}+\Psi^{\star}_{m_x,\ldots}\Psi_{m_x-1,\ldots}+\cdots)-\frac{k^2}{2}\sum_{m_x,\ldots}|\Psi_{m_x,\ldots}|^4. \tag{16}$$

Substituting the trial function (14) into Eq. (16) and using the fact that

$$-\sum_{m_x,\ldots}(\Psi^{\star}_{m_x,\ldots}\Psi_{m_x+1,\ldots}+\Psi^{\star}_{m_x,\ldots}\Psi_{m_x-1,\ldots}+\cdots)=\sum_{m_x,\ldots}(|\Psi_{m_x+1,\ldots}-\Psi_{m_x,\ldots}|^2+\cdots)-2d$$

for $d=1,2,3$, respectively, we finally obtain the expressions for the variational energy Φ,

$$\Phi(\eta)=-4d\frac{\eta}{1+\eta^2}-\frac{k^2}{2}\frac{(1-\eta^2)^d(1+\eta^4)^d}{(1+\eta^2)^{3d}},\quad d=1,2,3. \tag{17}$$

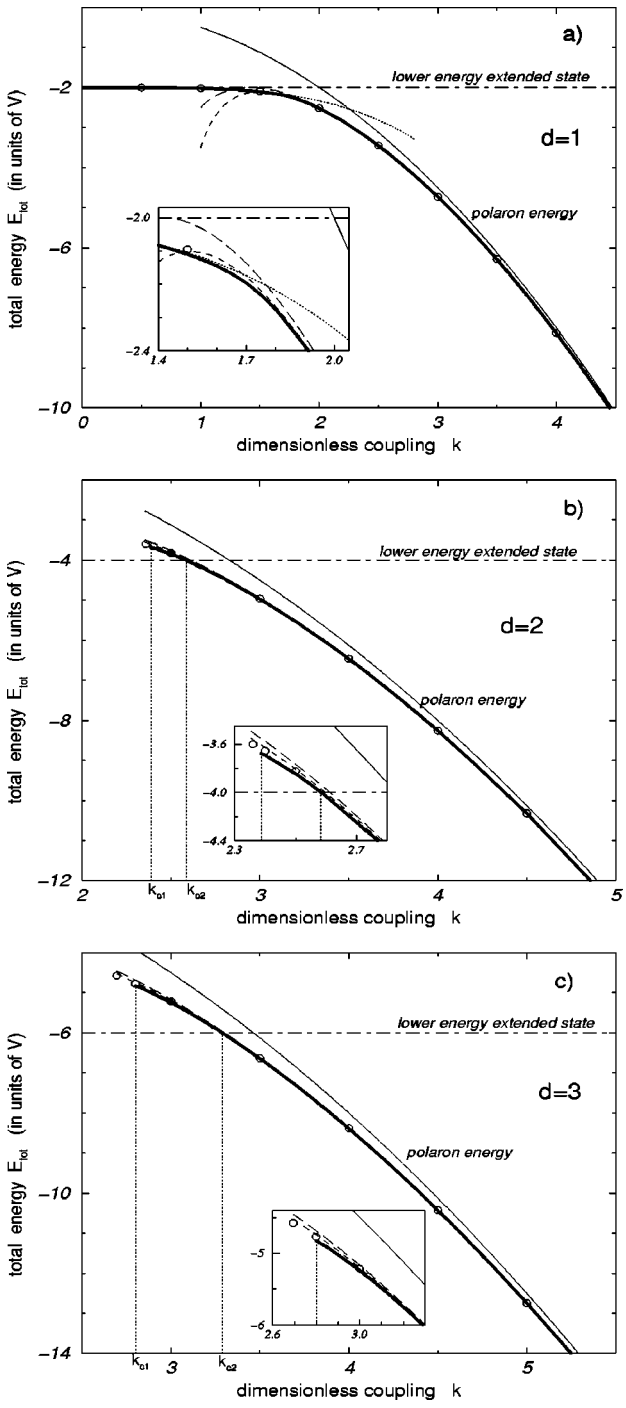

FIG. 1. Polaron total energy as a function of the dimensionless coupling (thick line) for simple lattices in (a) one dimension, (b) two dimensions, and (c) three dimensions. The open circles result from the numerical calculation of the minimum variational energy. The long-dashed lines are analytical expressions [Eq. (19)] that were obtained keeping in the variational minimum calculation only the first-order terms of the variational parameter. The short-dashed lines are more accurate expressions [Eq. (21)] resulting from a perturbation expansion of the variational parameter. The continuous thin lines show the zeroth-order result $-k^2/2$. The long-dash–short-dashed lines show the lowest energy of the extended states. The dotted line in (a) is the result of the continuous approximation. The critical values of coupling k_{c_1} and k_{c_2}, for $d=2$ and $d=3$, are also indicated in (b) and (c), respectively. In the insets we show in detail the transition regions.

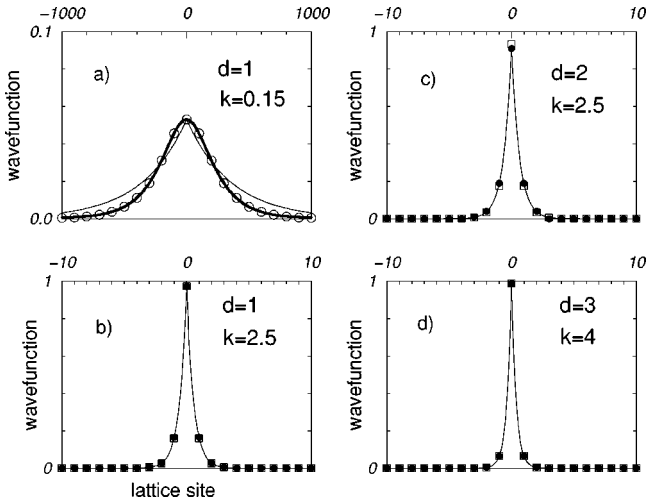

FIG. 2. Polaron wave functions. (a) The thick line shows a large polaron in 1D for $k=0.15$, the thin line results from the numerical calculation of the minimum of variational energy, and the open circles are values given by the continuous approximation. (b) The filled circles show a small polaron in 1D for $k=2.5$, the continuous line results from the numerical calculation of variational energy minimum, and the open squares are obtained analytically by the perturbation expansion of the variational parameter in the calculation of the variational minimum [Eqs. (20) and (14)]. (c) and (d) Sections of the polaron in 2D for $k=2.5$ and in 3D for $k=4$, respectively. The points and the lines have the same meaning as in (b).

In Figs. 3(a)–3(c) we show, for $d=1$, 2, and 3, respectively, the function $\Phi(\eta)$ for different values of the coupling k. The dashed lines show the lowest energy extended states. The variational energy (17) predicts qualitatively the existence of the critical values k_{c_1} and k_{c_2} in two and three dimensions and in one dimesnion the polaron exists for all the nonzero values of k, while there is a continuous transition from the small to the large polaron. In particular, for the three-dimensional case [Fig. 3(c)], for large k the minimum of $\Phi(\eta)$ is below the energy of the extended states and thus the polaron is the ground state. Furthermore, from Eq. (17), for $d=3$ we have that when $\eta\rightarrow 1$ the energy Φ goes to -6 as $-6+3(1-\eta)^2$, i.e., from above. This means that the extended state is a metastable state in this region of k, separated by an energy barrier from the polaron ground state. On the other side, for small k there is no minimum corresponding to a localized state. In the intermediate k region there is a minimum for $\eta<1$, but it corresponds to a metastable state since the absolute minimum corresponds to an extended state (at $\eta=1$). In 2D we see from Fig. 3(b) a similar behavior, even though there is one difference concerning the region of k where the polaron is the ground state. Specifically, for $d=2$ Eq. (17) gives that when $\eta\rightarrow 1$ the variational energy goes to -4 as $-4+(2-k^2/8)(1-\eta)^2$, i.e., from above when $k<4$ and from below when $k>4$. This means that for $k>4$ the extended state is unstable, while for $k<4$ it is metastable and has to overcome an energy barrier before falling to the polaron ground state. On the contrary, in the three-dimensional case, the energy barrier between the two solutions exists for all values of k. This feature was already noticed in Ref. 10, even though a different value of k, less than 4, was given for the vanishing of the barrier in 2D. The

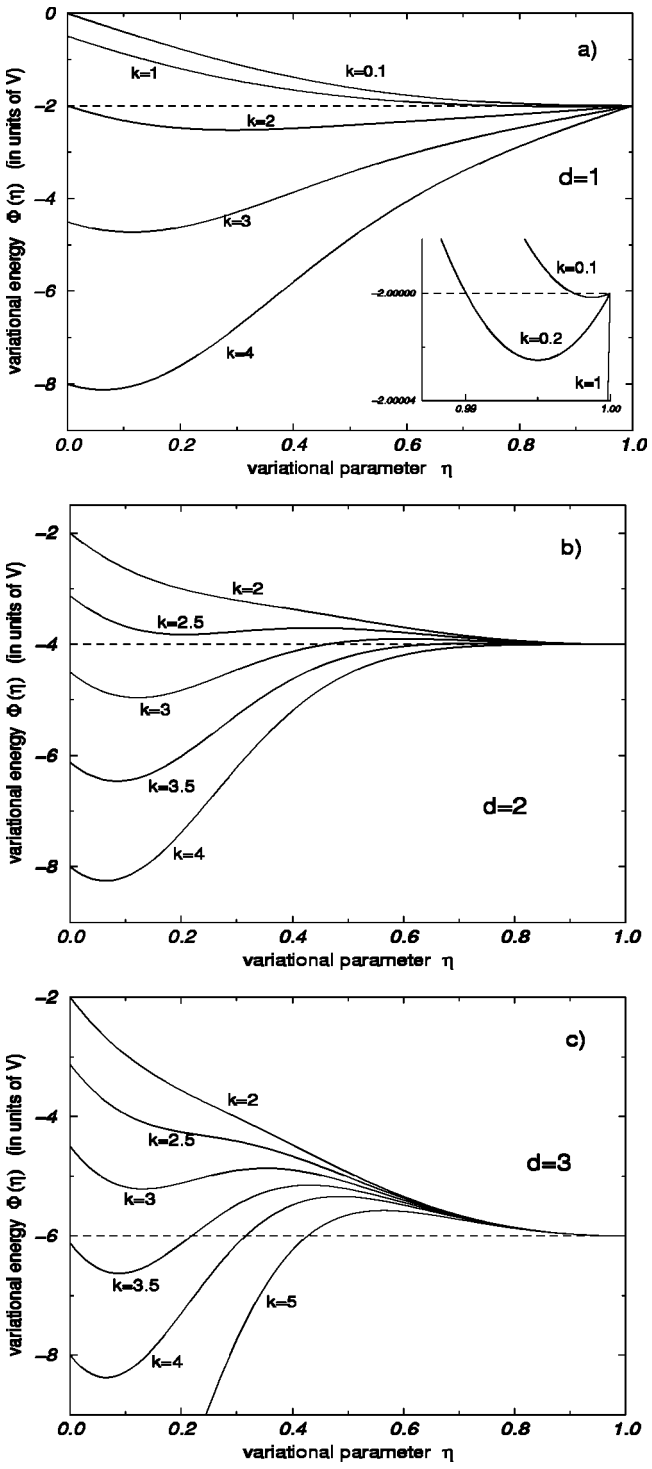

FIG. 3. Variational energy $\Phi(\eta)$ as a function of the variational parameter η, for different values of dimensionless coupling k, in (a) one dimension, (b) two dimensions, and (c) three dimensions. The dashed line in all cases shows the lowest energy of the extended states. The inset in (a) is an enlargement of the region close to $\eta=1$.

linear stability of the lowest energy extended state in two dimensions was numerically investigated using the method of a time Fourier transform of small oscillations around the solution (see Sec. V). The solution is unstable for k larger than a value that increases with the lattice size, but it seems to be saturated somewhere above 4.4 (at least for the lattice sizes that we were able to explore).[32] We note that the minimum of the variational energy in 2D and 3D corresponding to a localized solution is obtained for relatively small values of the variational parameter. This designates the formation of a small polaron. Contrary to the results in two and three dimensions, Fig. 3(a) shows qualitatively different results for the one-dimensional case. A minimum of the variational energy exists always below the energy of the extended states, even for very small k [see the inset of Fig. 3(a)]. As k decreases, the minimum becomes closer to the extended state energy, which is obtained for larger values of η. As a result, $k_{c_1}=0$ for $d=1$, since for $k=0$ there is no localized solution for the tight binding electron of Eq. (12). Furthermore, since the polaron solution is always the ground state, there is no second critical value k_{c_2}. For $d=1$ the function $\Phi(\eta)$ approaches -2 as $-2-(k^2/4)(1-\eta)$, i.e., always from below, resulting in unstable extended states.

We now present quantitative results of the variational approximation, as well as their agreement with the numerical results of Sec II A. From Eq. (17) we have $d\Phi/d\eta = P(\eta)[k^2-f(\eta)]$, where $P(\eta)$ is a positive function in the interval $0<\eta<1$ (different for each dimension) and the function $f(\eta)=f_d(\eta)$ (also positive in this interval) is given below. The minimization condition for the variational energy results in the equality

$$k^2=\frac{(1+\eta^2)^{3d-1}}{\eta(\eta^4-\eta^2+1)(1+\eta^4)^{d-1}(1-\eta^2)^{d-2}}\equiv f(\eta) \quad \text{for } d=1,2,3. \tag{18}$$

The function $f(\eta)$ determines the minimum of $\Phi(\eta)$ and consequently the polaron solutions. A straightforward calculation of the minima of the function $f(\eta)$ leads to the exact calculation of the critical coupling $k_{c_1}^{var}$ in two[33] and three dimensions. Furthermore, by substituting the k^2 from Eq. (18) into Eq. (17) and equating the $\Phi(\eta)$ with the lower energy of extended states, we obtain the corresponding values of η and from them the critical values $k_{c_2}^{var}$. These results, together with a comparison with the results obtained throught the numerical evaluation of Sec. II A are displayed in Table I. We observe good agreement between the analytical and numerical results.

In the following we derive expressions for the polaron energy. First, we observe that the numerical calculation of the minima of the variational energy (17) gives results for the energy and wave function in quite good agreement with the numerical solutions of Sec. II A [we compare the open circles in Figs. 1(a)–1(c), for the energy in each dimension and the continuous lines in Fig. 2 for the wave functions]. We also see that in 2D and 3D as well as for relatively large k in 1D, the minima of the variational energy are found at small values of the variational parameter η. As a result, it is possible to solve the minimization condition (18) keeping only first order terms of η. Then we find $\eta(k)=1/k^2$ for each dimension. Substituting the solution $\eta(k)$ into the variational energy (17), we obtain

$$\Phi_{var}=-\frac{k^2}{2}-\frac{2d}{k^2} \quad \text{for } d=1,2,3. \tag{19}$$

TABLE I. Comparison of the numerically, calculated, critical values of coupling with the corresponding analytical value derived through the variational method. NA denotes not available.

Dimension d	k_{c_1}	$k_{c_1}^{var}$	Relative error (%)	k_{c_2}	$k_{c_2}^{var}$	Relative error (%)
1	0	0		NA	NA	
2	2.3877	2.353	1.45	2.5844	2.593	0.33%
3	2.8022	2.694	3.85	3.2887	3.293	0.13%

These energies are presented in Figs. 1(a)–1(c) by the long-dashed lines (slightly above the thick lines of the numerical calculation). We note that the result (19) can be obtained by using more complicated diagrammatic technique.[34]

If we apply a perturbation expansion of $\eta(k)$ with respect to powers of $1/k^2$ we find from Eq. (18) that

$$\eta(k)=\frac{1}{k^2}+\frac{4d-2}{k^6}+O\left(\frac{1}{k^{10}}\right) \quad \text{for } d=1,2,3. \tag{20}$$

Substituting the expression (20) into Eq. (17), we obtain the results for the variational energy

$$\Phi_{var}=-\frac{k^2}{2}-\frac{2d}{k^2}-\frac{4d^2-3d}{k^6}+O\left(\frac{1}{k^{10}}\right) \quad \text{for } d=1,2,3. \tag{21}$$

In Figs. 1(a)–1(c) we plot these relations using short-dashed lines (between the thick and the long-dashed lines) for $d=1$, 2, and 3, respectively. We see that expression (21) approximates quite well the polaron energies in 2D and 3D (especially in the region where the polaron is the ground state, i.e., for $k>k_{c_2}$) and in 1D in the small polaron regime. The larger k is, the better the coincidence is. In the limit of very large k all the above-derived expressions tend to $-k^2/2$, reproducing the well-known result of the non-integrable limit.[1,9] The curves of $-k^2/2$ are also plotted for comparison in Figs. 1(a)–1(c) with the continuous thin lines. The results of Eqs. (19) and (20) in the one-dimensional case differ from the correspondig ones of Ref. 29 because in the latter paper the effect of the normalization of the electronic wave function on the depth of the lattice distortion was not taken into account.

The only case where the formula (21) fails to describe the polaron energy is in the one-dimensional large polaron, where η is relatively large. In this regime, however, the continuous approximation is valid, resulting in the solution[1]

$$\Psi_n=\frac{k}{2\sqrt{2}}\frac{1}{\cosh\left(\frac{k^2}{4}n\right)}, \tag{22}$$

with energy

$$\Phi_{cont}=-2-\frac{k^4}{48}. \tag{23}$$

The energy (23) is also shown, as a dotted line, in Fig. 1(a). We observe that it describes the polaron energy in almost the entire region where Eq. (21) for $d=1$ fails. We conclude that accurate analytical expressions of the polaron energy are available for almost all the values of coupling in one, two, and three dimensions.

The results for the wave functions are presented in Fig. 2. The open squares in Figs. 2(b)–2(d) show the variational wave functions of Eq. (14) with the parameter η given by Eq. (20). Figure 2(c) shows one of the worst approximated cases in 2D and 3D, viz., the metastable polaron (for $k_{c_1}<k<k_{c_2}$). In Fig. 2(a) the open circles show values given by the continuous approximation (22) that approximates accurately the large polaron.

III. NORMAL-MODES OF POLARONS

A. Born-Oppenheimer approximation

In order to study normal-modes of polarons, we consider the effects of small perturbations and linearize the equations of motion around the polaron solutions. We first treat this problem through the use of the Born-Oppenheimer approximation. We consider the oscillator displacements u_k for $k=1,\ldots,N$ as fixed parameters with the electron instantaneously adjusting. This is a good approximation when $\gamma \ll 1$. The electronic energy and wave function obey the equation

$$-\left(\sum_{\delta[i]}\Psi_{i+\delta}\right)+ku_i\Psi_i=E\{u_k\}\Psi_i, \tag{24}$$

while the dynamical equation for the oscillators is

$$\frac{d^2u_i}{d\tau^2}+u_i+\frac{\partial E\{u_k\}}{\partial u_i}=0. \tag{25}$$

We consider small deviations $\delta_i(\tau)$ from the polaron, i.e., $u_i(\tau)=u_i^0+\delta_i(\tau)$, where u_i^0 are the static polaron displacements. Substituting into Eq. (25) and using the Taylor expansion for the term $\partial E\{u_k\}/\partial u_i$, we get to first order for $\delta_i(\tau)$

$$\frac{d^2\delta_i}{d\tau^2}+\sum_j\,(J_{ij}+\delta_{ij})\,\delta_j(\tau)=0, \tag{26}$$

where $J_{ij}=\partial^2E\{u_k\}/\partial u_j\partial u_i$ and δ_{ij} is Kronecker's delta symbol.

The matrix elements J_{ij} can be computed through a numerical calculation of the second derivative since it is possible to find from Eq. (24) the values of E for u_i close to u_i^0.[32] However, a more accurate calculation can be done using perturbation theory. In particular, from Eq. (24) we have that $\partial E/\partial u_i=k\Psi_i^2$. Then $J_{ij}=2k\Psi_i(\partial\Psi_i/\partial u_j)$. In order to calculate $\partial\Psi_i/\partial u_j$, we find the first-order correction in the polaron wave function ϕ_i^0, using as a perturbation the δ_i's. As a result, we obtain

$$J_{ij}=-2k^2\phi_i^0\phi_j^0\sum_{\nu\neq 0}\,\frac{\phi_i^\nu\phi_j^\nu}{E_\nu-E_0}, \tag{27}$$

where the label ν counts the eigenfunctions of the unperturbed problem:

$$-\left(\sum_{\delta[i]} \phi^{\nu}_{i+\delta}\right)+ku_i^0\phi_i^{\nu}=E_{\nu}\phi_i^{\nu}. \tag{28}$$

The ground state $\nu=0$ corresponds to the polaron. Thus, from the diagonalization of the unperturbed Hamiltonian $H_{0_{ij}}=ku_i^0\delta_{ij}-(\delta_{i,j+1}+\delta_{i,j-1})$ we compute the matrix J_{ij} using the sum (27). From Eq. (26) we see that in order to find the normal modes we have to diagonalize the matrix $J_{ij}+\delta_{ij}$. The resulting eigenvalues give the square of the eigenfrequencies.

In Figures 4(a)–4(c) we present the five lowest eigenfrequencies as a function of the coupling k for $d=1$, 2, and 3, respectively. All other eigenfrequencies are conjested between these five and the frequency ω_0 of the oscillators. The corresponding eigenvectors of the four lowest modes for $d=1$ and 2 are shown in Fig. 5. In 1D for large k (in the small polaron region) the lower mode is a breathing symmetric mode [see Fig. 5(a)] and the next mode is an antisymmetric pinning mode [see Fig. 5(b)]. As can be seen from Fig. 5(a), when k decreases there is a mode crossing and the pinning mode becomes the lower one. This happens in the region of the transition from the small to the large polaron. For smaller k the pinning mode squared frequency is very small (close to zero), but positive. We note that if a squared frequency is zero or negative then the solution is unstable. This is not the case for the one-dimensional polaron. In 2D and 3D the lowest mode is always a breathing mode [see Fig. 5(e) for $d=2$]. Its frequency goes abruptly to zero as the critical value k_{c_1} is approached. The next higher frequency is a pinning mode and it is doubly degenerate in 2D [see Figs. 5(f) and 5(g)] while triply degenerate in 3D. These degenerate modes correspond to perpendicular directions. The renormalization of the phonon frequencies has also been found in a small cluster consisting of four sites.[8,11]

B. Study of the complete problem

In order to study the complete problem we depart from the Born-Oppenheimer approximation and take additionally into account the electronic motion. For small perturbations from the polaron solutions u_i^0 and ϕ_i^0 we have

$$\Psi_i(\tau)=[\phi_i^0+\epsilon_i(\tau)]e^{-i(E_0/\gamma)\tau},$$

$$u_i(\tau)=u_i^0+\delta_i(\tau), \quad i=1,2,\ldots,N, \tag{29}$$

where $\epsilon_i(\tau)$ is complex and $\delta_i(\tau)$ and $|\epsilon_i(\tau)|$ are very small. Substituting into Eqs. (6) and (7) and keeping first-order terms in δ_i and ϵ_i, we obtain the linearized equations

$$-\left(\sum_{\delta[i]} \epsilon_{i+\delta}\right)+(ku_i^0-E_0)\epsilon_i+k\phi_i^0\delta_i=i\gamma\frac{d\epsilon_i}{d\tau},$$

$$\frac{d^2\delta_i}{d\tau^2}+k\phi_i^0(\epsilon_i+\epsilon_i^{\star})+\delta_i=0. \tag{30}$$

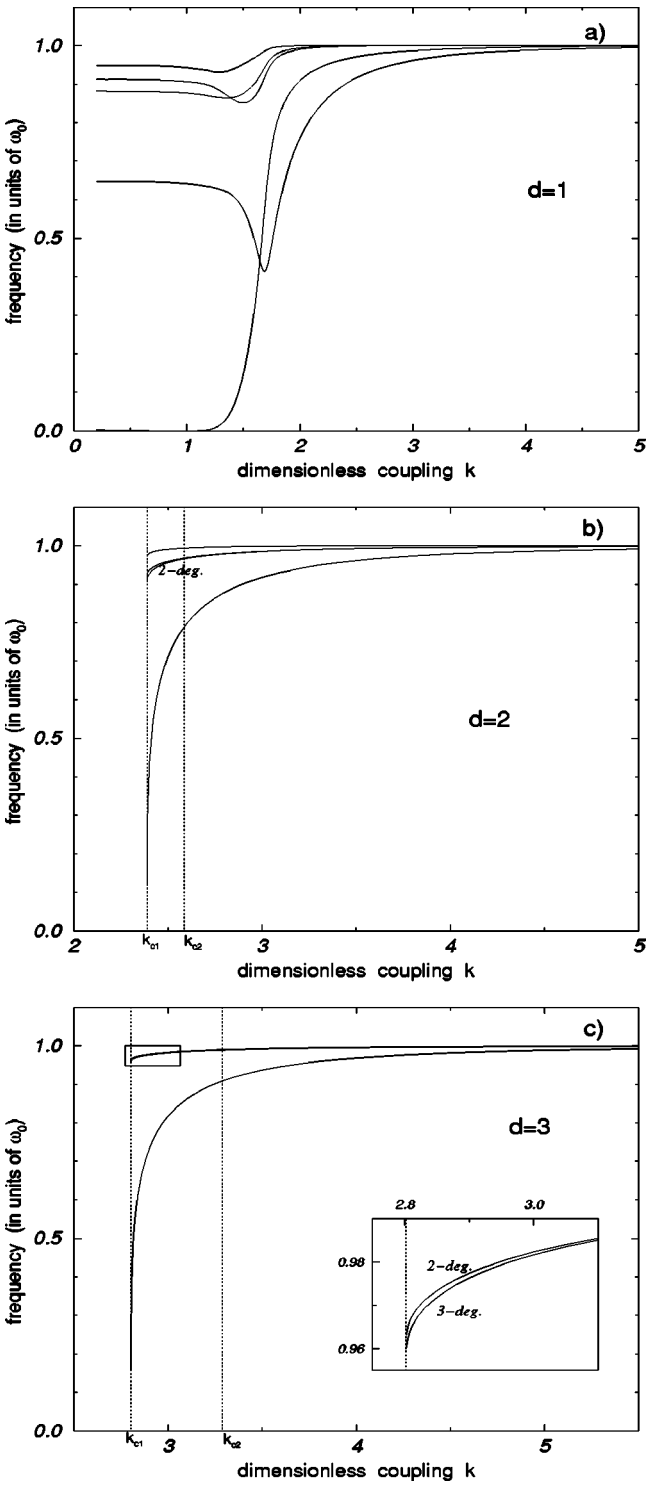

FIG. 4. The five lowest polaron eigenfrequencies in the Born-Oppenheimer approximation as a function of the coupling for (a) one dimension, (b) two dimensions, and (c) three dimensions. We note a mode crossing in the one-dimensional case, at the transition regime from a small to a large polaron.

There are two ways to proceed. The polaron solution is periodic in the $4N$-dimensional phase space of $\{\mathrm{Re}\,\Psi_i,\mathrm{Im}\,\Psi_i,u_i,\dot{u}_i\}$ with period $T=2\pi\gamma/E_0$ (because $\Psi_i(\tau)=\phi_i^0e^{-i(E_0/\gamma)\tau}$). A standard way for finding the normal modes in this case is by using the Floquet analysis. For this we have to calculate numerically the tangent map M and

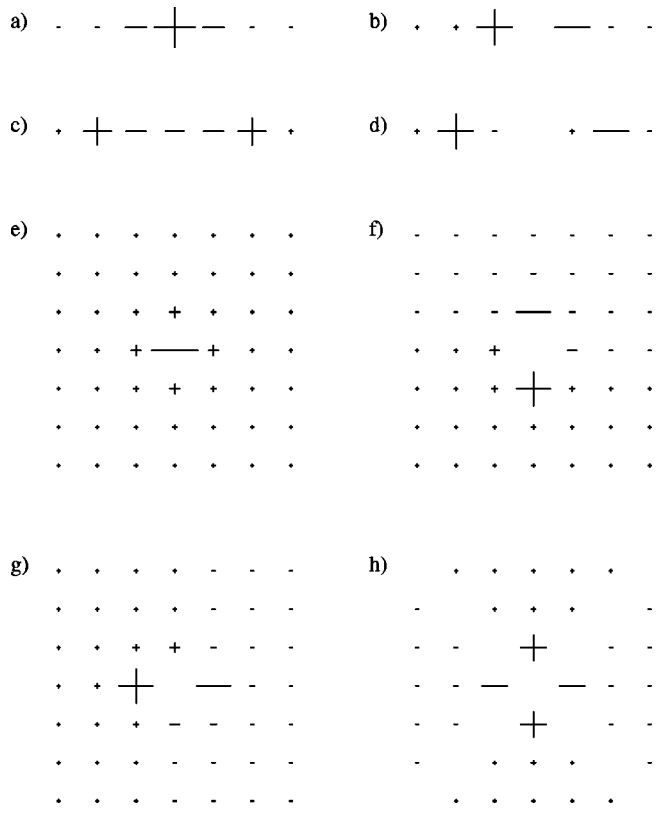

FIG. 5. The four lowest eigenmodes of the polaron in the Born-Oppenheimer approximation (a)–(d) in one dimension for $k=2.5$ and (e)–(h) in two dimensions for $k=2.5$. The sign of the corresponding eigenvector at each lattice site is presented with a size proportional to its magnitude. A zero value in the eigenvector is represented by an empty site.

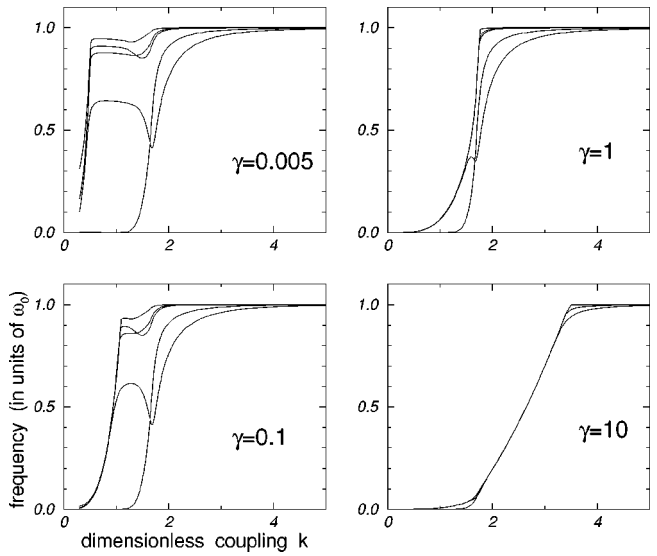

FIG. 6. The five lowest polaron eigenfrequencies as a function of the coupling for different values of γ in a one-dimensional lattice consisting of $N=500$ sites.

diagonalize it. The latter maps an initial deviation $\{\mathrm{Re}\,\epsilon_i(0),\mathrm{Im}\,\epsilon_i(0),\delta_i(0),\dot{\delta}_i(0)\}$ from the periodic solution to a deviation resulting from the linearized equations (30) after a period T, i.e., $\{\mathrm{Re}\,\epsilon_i(T),\mathrm{Im}\,\epsilon_i(T),\delta_i(T),\dot{\delta}_i(T)\}=M\{\mathrm{Re}\,\epsilon_i(0),\mathrm{Im}\,\epsilon_i(0),\delta_i(0),\dot{\delta}_i(0)\}$. Due to the normalization condition $\Sigma_i|\Psi_i|^2=1$, implying $\Sigma_i\phi_i^0\,\mathrm{Re}\,\epsilon_i=0$, the dimension of the map that will be diagonalized is $(4N-1)\times(4N-1)$. We do not present here the results of the Floquet analysis for the polarons,[32] but continue the analysis using the time Fourier transform method, which also permits us to obtain the polaron normal modes.

We consider $\delta_i(\tau)=\delta_i(\omega)\cos\omega\tau$ and $\epsilon_i(\tau)=\epsilon_i^{(1)}(\omega)\cos\omega\tau+i\epsilon_i^{(2)}(\omega)\sin\omega\tau$ and use $\epsilon_i^{(1),(2)}(\omega)=\Sigma_\nu\epsilon_\nu^{(1),(2)}(\omega)\phi_i^\nu$, where the ϕ_i^ν are the eigenfunctions of Eq. (28) obeying $\Sigma_i\phi_i^\nu\phi_i^{\nu'}=\delta_{\nu\nu'}$; after substitution into Eqs. (30) we obtain the system of equations

$$\left(E_\nu-E_0-\frac{\omega^2\gamma^2}{E_\nu-E_0}\right)\epsilon_\nu^{(1)}(\omega)+k\sum_i\phi_i^0\phi_i^\nu\delta_i(\omega)=0 \qquad \forall\,\nu\neq 0,$$

$$k\sum_{\nu\neq 0}\phi_i^0\phi_i^\nu\epsilon_\nu^{(1)}(\omega)+\frac{1}{2}(1-\omega^2)\delta_i(\omega)=0 \quad \forall i. \tag{31}$$

We have additionally that for $\nu\neq 0$, $\epsilon_\nu^{(2)}(\omega)=-[\omega\gamma/(E_\nu-E_0)]\epsilon_\nu^{(1)}(\omega)$, whereas for $\nu=0$ the values are $\epsilon_{\nu=0}^{(1)}(\omega)=0$ [this relation is equivalent with the normalization condition for the Ψ_i of Eq. (29)] and $\epsilon_{\nu=0}^{(2)}(\omega)=-(k/\omega\gamma)\Sigma_i\phi_i^0\delta_i(\omega)$.

For nonzero solutions the determinant of the system (31) should be equal to zero. Thus the eigenfrequencies will be obtained through the condition

$$\det(\Pi)=\det\begin{pmatrix}A & R\\ R^T & C\end{pmatrix}=0, \tag{32}$$

where A is an $(N-1)\times(N-1)$ diagonal matrix with elements $A_{\nu\nu'}=\{E_\nu-E_0-[\omega^2\gamma^2/(E_\nu-E_0)]\}\delta_{\nu\nu'}$, R is the $(N-1)\times N$ matrix $R_{\nu i}=k\phi_i^0\phi_i^\nu$, R^T is its transpose, and C is $N\times N$ diagonal $C_{ij}=\frac{1}{2}(1-\omega^2)\delta_{ij}$.

We note that in the limit $\gamma=0$ the condition (32) reduces to the Born-Oppenheimer result. This is seen clearly by using

$$\det(\Pi)=\det(A)\det(C-R^TA^{-1}R) \tag{33}$$

and

$$(C-R^TA^{-1}R)_{ij}=\frac{1}{2}\left[(1-\omega^2)\delta_{ij}-2k^2\sum_{\nu\neq 0}\frac{\phi_i^0\phi_i^\nu\phi_j^0\phi_j^\nu}{E_\nu-E_0-\dfrac{\omega^2\gamma^2}{E_\nu-E_0}}\right], \tag{34}$$

where in the limit $\gamma=0$ the last term gives the J_{ij} of Eq. (27). For $\gamma\neq 0$, after multiplications of the first $N-1$ lines and columns of Π by $\sqrt{E_\nu-E_0}/\gamma$ and the last N lines and columns by $\sqrt{2}$, we obtain the squared eigenfrequencies from the diagonalization of the matrix

$$\begin{pmatrix} \left(\frac{\Delta E_1}{\gamma}\right)^2 & \cdots & 0 & \frac{\sqrt{2}k}{\gamma}\phi_1^0\phi_1^1\sqrt{\Delta E_1} & \cdots & \frac{\sqrt{2}k}{\gamma}\phi_N^0\phi_N^1\sqrt{\Delta E_1} \\ 0 & \cdots & 0 & \frac{\sqrt{2}k}{\gamma}\phi_1^0\phi_1^2\sqrt{\Delta E_2} & \cdots & \frac{\sqrt{2}k}{\gamma}\phi_N^0\phi_N^2\sqrt{\Delta E_2} \\ \vdots & & \vdots & \vdots & & \vdots \\ 0 & \cdots & \left(\frac{\Delta E_{N-1}}{\gamma}\right)^2 & \frac{\sqrt{2}k}{\gamma}\phi_1^0\phi_1^{N-1}\sqrt{\Delta E_{N-1}} & \cdots & \frac{\sqrt{2}k}{\gamma}\phi_N^0\phi_N^{N-1}\sqrt{\Delta E_{N-1}} \\ \frac{\sqrt{2}k}{\gamma}\phi_1^0\phi_1^1\sqrt{\Delta E_1} & \cdots & \frac{\sqrt{2}k}{\gamma}\phi_1^0\phi_1^{N-1}\sqrt{\Delta E_{N-1}} & 1 & \cdots & 0 \\ \vdots & & \vdots & \vdots & & \vdots \\ \frac{\sqrt{2}k}{\gamma}\phi_N^0\phi_N^1\sqrt{\Delta E_1} & \cdots & \frac{\sqrt{2}k}{\gamma}\phi_N^0\phi_N^{N-1}\sqrt{\Delta E_{N-1}} & 0 & \cdots & 1 \end{pmatrix}, \quad (35)$$

where ΔE_ν stands for the difference $E_\nu - E_0$.

In Fig. 6 we present for different γ the five lowest eigenfrequencies as a function of k in one dimension. We observe that for relatively large k the lower modes are determined essentially by the lattice thus reproducing the Born-Oppenheimer results. For small k, however, the electronic motion modifies this picture. Depending on γ, a transition takes place at different values of k. The smaller the γ, the smaller the corresponding transition value k_t. Similar behavior appears in two and three dimensions. However, since there is no polaron for $k<k_{c_1}$, there is no such transition at all for relatively small γ ($\leqslant 1-2$).

We calculate the electronic contribution at each eigenvector through the ratio $\Sigma_\nu[(\epsilon_\nu^{(1)})^2+(\epsilon_\nu^{(2)})^2]/\{\Sigma_i\delta_i^2+\Sigma_\nu[(\epsilon_\nu^{(1)})^2+(\epsilon_\nu^{(2)})^2]\}$. We see that the character of the lower modes changes abruptly from phononic to electronic at the transition point k_t. The character of lower modes is interpreted by the position of the spectrum of electronic frequencies $(E_\nu-E_0)/\gamma$ with respect to the frequency 1 (in our dimensionless units) of the pure lattice. In particular, as can be seen from the matrix (35), we couple the N phonon frequencies at a frequency equal to 1 with the $N-1$ electronic frequencies. For fixed k, the smaller the γ, the higher the frequencies $(E_\nu-E_0)/\gamma$. For fixed γ, the larger the k, the higher the excitation energies $E_\nu-E_0$ of the eigenvalue equation (28) and, as a result, the higher the electronic frequencies. When the electronic spectrum is far away from frequency 1, due to the coupling, some phonon frequencies split from the others. This results in lower modes with phononic character that can be accurately provided by the Born-Oppenheimer approximation. As long as the electronic spectrum remains above the unit frequency the lattice determines the lower modes. Increasing γ or decreasing the coupling k changes abruptly the character of the lower modes and the transition takes place when the electronic spectrum crosses the Born-Oppenheimer phonon frequencies.

The density of states (DOS) of the spectrum of polaron eigenfrequencies consists of a thin and very strong, δ-like peak at frequency 1 plus a band with an electronic origin. The position of the band depends on k and γ, as discussed previously, while its width is $4d/\gamma$, where d is the lattice dimensionality. The only important effect of the interaction is the appearance of several discrete phononic levels that are visible if not covered by the band. If the electronic band is above (below) the unit then the disjoin phononic levels are below (above) the strong peak. In Fig. 7 we present the DOS of polaron eigenfrequencies together with the DOS of the electronic spectrum $(E_\nu-E_0)/\gamma$ for $\gamma=10$ and two different values of k, in two dimensions. Qualitatively, the only difference in the total picture of the spectrum at the other dimensions is the shape of the electronic band. For example, in one dimension there exist very strong peaks in the band edges, as a square root singularity.[35]

The electronic frequencies $(E_\nu-E_0)/\gamma$ and thus the location of the electronic band as a function of the parameters k and γ can be evaluated analytically. The lower band edge of the electronic frequencies is determined from the expression

$$\omega_{band}=\frac{-2d-E_0}{\gamma}, \quad (36)$$

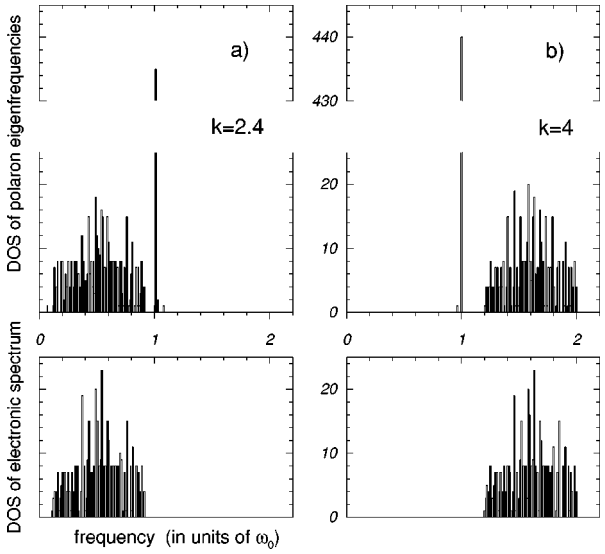

FIG. 7. Density of states (DOS) of polaron eigenfrequencies and also of the electronic spectrum in a two-dimensional lattice consisting of $N=21\times 21$ sites for $\gamma=10$ and (a) $k=2.4$ and (b) $k=4$.

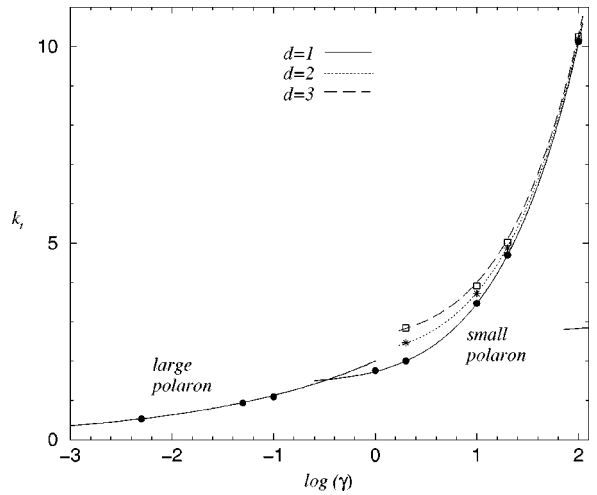

FIG. 8. Critical value of coupling k_t for which the transition of the lower normal modes from phononic to electronic takes place as a function of the logarithm (base 10) of γ. The lines are the analytical results. The filled circles show the numerical results for one dimension, the asterisks for two dimensions, and the empty squares for three dimensions.

where E_0 is the ground state of Eq. (28). We obtain different expressions for the small and large polaron, respectively, using the result $E_0=-k^2$ in the first case and $E_0=-2-k^4/16$ in the second. For the small polaron case E_0 is obtained through Eq. (17) with the substitution of $k^2/2$ with k^2, while the dependence of $\eta(k)$ will remain the same. The reason is that Eq. (17) includes also the lattice energy, which we substrate by using, for the static solution, that $E_{int}=-2E_{lat}$ holds. Finally, we have for the small polaron

$$\omega_{band}=\frac{k^2-2d}{\gamma}, \quad d=1,2,3 \tag{37}$$

and for the large polaron for $d=1$

$$\omega_{band}=\frac{k^4}{16\gamma}. \tag{38}$$

If we use the more accurate expression (20) for the $\eta(k)$ of the small polaron, we obtain an additional term $-2d(4d-3)/k^6$ in the nominator of Eq. (37). At large k values the electonic spectrum and the phononic peak at $\omega_0=1$ are well separated; as the value of the coupling is reduced the spectra come closer and at some critical value k_t the character of the lower modes changes from phononic to electronic. This point is determined through the condition $\omega_{band}(k_t)\approx 1$. As a result we obtain for the small polaron

$$k_t=\sqrt{\gamma+2d}, \quad d=1,2,3 \tag{39}$$

and for the large polaron for $d=1$

$$k_t=2(\gamma)^{1/4}. \tag{40}$$

The dependence of k_t on γ is depicted in Fig. 8, where the continuous curves are the analytical results of Eqs. (39) and (40) and the discrete points represent numerical results.

IV. CONCLUSIONS

We studied the polaron solutions of the semiclassical Holstein model in one, two, and three dimensions. The classical treatment of the lattice permits us to obtain dynamical equations suitable for numerical integrations. The stationary solutions of these equations can be either extended Bloch states or localized polarons. Using a very simple numerical method we are able to calculate the polaron energies and wave functions for all values of the parameters. In two and three dimensions there are two critical values of the dimensionless coupling k. For $k<k_{c_1}$ there are no polaron solutions, while for $k>k_{c_2}$ the polaron is the ground state of the system. In the two-dimensional square lattice the critical values are $k_{c_1}=2.3877$ and $k_{c_2}=2.5844$, while in the three-dimensional simple cubic lattice they are $k_{c_1}=2.8022$ and $k_{c_2}=3.2887$. In contrast, in one dimension the polaron solution is always the ground state. These qualitative results are not restricted to the simple lattices that we have considered in our work. For example, if we apply our numerical method to the two-dimensional honeycomb lattice (the structure of graphite) we find the same picture as in the square lattice, where now the critical values are $k_{c_1}=2.0345$ and $k_{c_2}=2.1465$, i.e., shifted downward. It seems quite reasonable that the smaller the coordination number, the easier it is for the electron to be trapped due to lattice deformation.

We applied a variational method approximating the polaron state by a simple trial function. Because of the simple form of the trial function we found explicitly the energy Φ as a function of the variational parameter. The dependence of Φ on the coupling constant explains qualitatively all the features of the polaron for each dimension. Furthermore, we are able to find exactly the critical values of coupling, which are in very good agreement with the numerically calculated values (Table I in Sec. IV). Although we cannot solve analytically the minimization condition, keeping leading terms appropriate for a small polaron, we derive exact formulas for the polaron energy, given by Eq. (19). Using a perturbation expansion, we derive expressions (21) that provide a better description of the polaron energy, especially close to the transitions regimes. These relations approximate accurately the numerical results in almost all the cases, except that of the large polaron in 1D where the continuous approximation is valid and its energy is given by Eq. (23).

Finally, the normal-modes of small perturbations around the polarons were examined. We presented the lower modes and the dependence of their frequency on the parameters of the model. We analyzed whether they have phononic or electronic character, i.e., if they are determined principally by the lattice or electron motion, respectively. In the former case they are fully described by the Born-Oppenheimer approximation. Their character depends on the position of the spectrum of electronic frequencies with respect to the frequency ω_0 of the Einstein oscillators. Moreover, the complete picture of the density of states of polaron eigenfrequencies was discussed. We derived analytical expressions for the lower edges of the electronic band and through them expressions for the critical value k_t that changes the character of the lower normal modes from phononic to electronic. We note that the normal-modes may be manifest in the spectra of real

systems described through the Holstein model.

The results presented in this work depend on the validity of the semiclassical approximation. The latter coincides with the adiabatic approximation in the limit of atoms with infinite mass. Several recent investigations have shown good ageement between exact diagonalization and approximate resuls in this regime.[10,11] On the other hand, it is known that semiclassical self-trapping[4] may not survive in an exact quantum lattice regime.[8] The atomic vibrational frequency sets the appropriate time scale during which the semiclassical results are valid. Consequently, the time regime of validity of the semiclassical results extends as the the mass of the atoms increases, while the general disparity of electronic and vibrational time scales sets the regime of validity of the approximation to times of the order of $1/\omega_0$.

ACKNOWLEDGMENTS

This work was supported by the European Union through the Marie-Curie Foundation (S.A.) through Grant No. ERBFMBICT2237 and by INTAS through Grant No. INTAS-96-158. G.K. acknowledges the warm hospitality of Laboratoire Léon Brillouin in Saclay and support through ΠΕΝΕΔ Grant No. 95-*E*Δ-115 from the General Secretariat of Research and Technology of Greece.

[1] T. Holstein, Ann. Phys. (N.Y.) **8**, 325 (1959).
[2] J. Appel, in *Solid State Physics*, edited by H. Ehrenreich and D. Turnbull (Academic, New York, 1968), Vol. 21, p. 193.
[3] D. Emin and T. Holstein, Phys. Rev. Lett. **36**, 323 (1976).
[4] D. Feinberg and J. Ranninger, Physica D **14**, 29 (1984).
[5] E. I. Rashba, in *Excitons*, edited by E. I. Rashba and D. M. Struge (Nauka, Moscow, 1985).
[6] H. Böttger and V. V. Bryksin, *Hopping Conduction in Solids* (Akademie-Verlag, Berlin, 1985).
[7] D. M. Alexander and J. A. Krumhansl, Phys. Rev. B **33**, 7172 (1986).
[8] J. Ranninger and U. Thibblin, Phys. Rev. B **45**, 7730 (1992).
[9] S. Aubry, in *Phase Separation in Cuprate Superconductors*, edited by K. A. Müller and G. Benedek (World Scientific, Singapore, 1993), p. 304.
[10] V. V. Kabanov and O. Yu. Mashtakov, Phys. Rev. B **47**, 6060 (1993).
[11] A. S. Alexandrov, V. V. Kabanov, and D. K. Ray, Phys. Rev. B **49**, 9915 (1994).
[12] A. S. Alexandrov and Nevill Mott, *Polarons & Bipolarons* (World Scientific, Singapore, 1995).
[13] E. de Mello and J. Ranninger, Phys. Rev. B **55**, 14 872 (1997).
[14] M. Capone, W. Stephan, and M. Grilli, Phys. Rev. B **56**, 4484 (1997).
[15] G. Wellein and H. Fehske, Phys. Rev. B **56**, 4513 (1997).
[16] J. M. Robin, Phys. Rev. B **56**, 13 634 (1997).
[17] E. N. Economou, O. Yanovitskii, and Th. Fraggis, Phys. Rev. B **47**, 740 (1993).
[18] A. V. Zolotaryuk, A. Mistriotis, and E. N. Economou, Phys. Rev. B **48**, 13 518 (1993).
[19] D. Chen, M. I. Molina, and G. P. Tsironis, J. Phys.: Condens. Matter **5**, 8689 (1993).
[20] G. Kopidakis, C. M. Soukoulis, and E. N. Economou, Phys. Rev. B **51**, 15 038 (1995).
[21] M.-N. Bussac, G. Mamalis, and P. Mora, Phys. Rev. Lett. **75**, 292 (1995).
[22] A. C. Scott, Phys. Rep. **217**, 1 (1992), and references therein.
[23] W. C. Kerr and P. S. Lomdahl, Phys. Rev. B **35**, 3629 (1987).
[24] A. V. Zolotaryuk, K. H. Spatschek, and O. Kluth, Phys. Rev. B **47**, 7827 (1993).
[25] A. V. Zolotaryuk, K. H. Spatschek, and A. V. Savin, Phys. Rev. B **54**, 266 (1996).
[26] J. C. Eilbeck, P. S. Lomdahl, and A. C. Scott, Physica D **16**, 318 (1985).
[27] M. I. Molina and G. P. Tsironis, Physica D **65**, 267 (1993).
[28] G. Kalosakas, G. P. Tsironis, and E. N. Economou, J. Phys.: Condens. Matter **6**, 7847 (1994).
[29] S. Aubry and P. Quemerais, in *Low-Dimensional Electronic Properties of Molybdenum Bronzes and Oxides*, edited by C. Schlenker (Kluwer Academic, Dordrecht, 1989), p. 295.
[30] S. Aubry, G. Abramovici, and J.-L. Raimbault, J. Stat. Phys. **67**, 675 (1992).
[31] S. Aubry, Physica D **71**, 196 (1994).
[32] G. Kalosakas, Ph.D thesis, University of Crete, Greece, 1997.
[33] G. Kalosakas, G. P. Tsironis, and S. Aubry, in *Nonlinear Klein-Gordon and Schrödinger Systems: Theory and Applications*, edited by L. Vázquez *et al.* (World Scientific, Singapore, 1996), p. 313.
[34] A. A. Gogolin, Phys. Status Solidi B **109**, 95 (1982).
[35] E. N. Economou, *Green's Functions in Quantum Physics* (Springer-Verlag, Berlin, 1990).